Sensitivity of Second Harmonic Generation from Styryl Dyes to Transmembrane Potential

Andrew C. Millard,* Lei Jin,* Mei-de Wei,* Joseph P. Wuskell,* Aaron Lewis,† and Leslie M. Loew*
*Department of Physiology and Center for Biomedical Imaging Technology, University of Connecticut Health Center, Farmington, Connecticut; and †Division of Applied Physics, Hebrew University, Jerusalem, Israel

ABSTRACT In this article we present results from the simultaneous nonlinear (second harmonic generation and two-photon excitation fluorescence) imaging and voltage clamping of living cells. Specifically, we determine the sensitivity to transmembrane potential of second harmonic generation by ANEP-chromophore styryl dyes as a function of excitation wavelength and dye structure. We have measured second harmonic sensitivities of up to 43% per 100 mV, more than a factor of four better than the nominal voltage sensitivity of the dyes under "one-photon" fluorescence. We find a dependence of voltage sensitivity on excitation wavelength that is consistent with a two-photon resonance, and there is a significant dependence of voltage sensitivity on the structure of the nonchromophore portion of the dyes.

INTRODUCTION

The discovery of voltage-dependent changes in the fluorescence of dyes staining the squid giant axon (Cohen et al,. 1974; Tasaki, 1974) was quickly applied to the study of the electrical properties of a variety of cell and membrane preparations (Freedman and Laris, 1981) and many new dyes have been developed for the purpose of imaging transmembrane potential (TMP). Styryl dyes are of considerable interest because they respond to changes in TMP by a fast, electrochromic mechanism (Loew et al., 1978, 1979; Loew and Simpson, 1981; Loew, 1982). The ANEP-based dyes, such as those shown in Fig. 1, exhibit such behavior. They consist of quaternized pyridinium electron acceptor moieties linked by a π-bond to amino-naphthalene electron donors (Hassner et al., 1984; Fluhler et al., 1985). The chromophore's positive charge is concentrated in the pyridine ring in the ground state and shifts to the amino-naphthalene in the excited state (Loew et al., 1978, 1979). This charge-shift couples with an electric field within a cell membrane, resulting in electrochromism. The *n*-alkyl groups are intended to orient the molecule in alignment with membrane lipids, approximately perpendicular to the membrane surface, maximizing sensitivity to TMP. The pyridinium nitrogen is a suitable site for an aqueous anchor, such as propylsulphonate, methylribofuraniside or methylpropanol as shown in Fig. 1, hindering transmembrane migration of the dye. The dyes are stable, whereas toxicity and photodynamic effects are low for most imaging applications. The success of di-4-ANEPPS as one of the most generally useful fast potentiometric dyes results from its remarkably consistent voltage sensitivity in a variety of systems (Loew et al., 1992). With a typical relative signal change of 10% per 100 mV, di-4-ANEPPS and its octyl analog are popular dyes for fluorescence imaging of TMP (Fluhler et al., 1985; Loew et al., 1992; Zhang et al., 1998).

The physical phenomenon of optical second harmonic generation (SHG) occurs when an intense laser beam interacts with a noncentrosymmetric polarizable material to produce coherent light at precisely half the incident wavelength. It is a nonlinear optical process with some features in common with two-photon excitation fluorescence (2PF) and has largely been developed as a technique for studying surfaces and interfaces (Shen, 1989; Eisenthal, 1996). Many of the approaches used to probe bulk material properties can be adapted for microscopy (Sheppard et al., 1977). Lewis and co-workers have developed resonance-enhanced SHG to obtain greater signal levels from dyes and natural chromophores (Huang et al., 1989), and we have used this technique to determine the voltage dependence of SHG from styryl dyes in hemispherical bilayers of oxidized cholesterol (Bouevitch et al., 1993; Ben-Oren et al., 1996). For the theory of SHG and its voltage sensitivity, see the review by Millard et al. (2003a).

In this article we are interested in the voltage sensitivity of 2PF and SHG from styryl dyes, though we shall also refer to the dyes' ''1PF'' or linear (one-photon) excitation fluorescence. An important difference between SHG and 2PF is that the former has constraints confining signal to regions lacking a center of symmetry (Shen, 1984; Boyd, 1992). These constraints are readily satisfied at mismatched interfaces (Shen, 1989), such as cell membranes in which one leaflet has been stained (Campagnola et al., 1999; Moreaux et al., 2000a,b). Any transfer of the dye to the other leaflet, or any irregularity in the cell membrane, may partially restore symmetry and reduce SHG. Some of our dyes, such as di-4-ANEPMRF and di-4-ANEPMPOH, also possess a chiral center that can sufficiently weaken the symmetry even in cases where dye has equilibrated between the two membrane leaflets, allowing SHG (Campagnola et al., 1999).

Most of the earlier work concerning SHG voltage-sensing has used nonbiological systems and/or indirect methods to

Submitted July 25, 2003, and accepted for publication September 29, 2003.
Address reprint requests to Leslie M. Loew, Center for Biomedical Imaging Technology, University of Connecticut Health Center, 263 Farmington Ave. MC-1507, Farmington, CT 06030-1507. Tel.: 860-679-3568; Fax: 860-679-1039; E-mail: les@volt.uchc.edu.

0006-3495/04/02/1169/08 $2.00

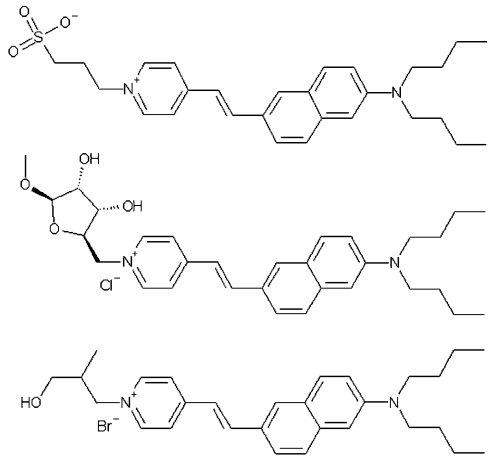

FIGURE 1 (*Top*) di-4-AminoNaphthenyl-PyridiniumPropylSulphonate or di-4-ANEPPS. (*Middle*) di-4-AminoNaphthenyl-PyridiniumMethyl-RiboFuranoside or di-4-ANEPMRF. (*Bottom*) di-4-AminoNapthenyl-PyridiniumMethylPropanol or di-4-ANEPMPOH.

manipulate TMP (Bouevitch et al., 1993; Ben-Oren et al., 1996; Campagnola et al., 1999; Peleg et al., 1999; Moreaux et al., 2003). In contrast, we determine the SHG voltage sensitivity of membrane-staining dyes by voltage clamping live cells in order to directly control TMP. Our initial work found a voltage sensitivity of 18%/100 mV for SHG from di-4-ANEPPS excited at 850 nm (Millard et al., 2003b). Here we report our investigations of the dependence of SHG voltage sensitivity on excitation wavelength as a means to tune resonance-enhancement and maximize the sensitivity. We have measured SHG voltage sensitivities up to 43%/100 mV—approximately four times better than the sensitivities that can be achieved with 1PF. We also screen other ANEP-based dyes as possible candidates for use in SHG voltage sensing.

MATERIALS AND METHODS

Imaging system

We have adapted a Fluoview scanning confocal imaging system (Olympus America, Melville, NY) for nonlinear optical imaging with an upright, stage-focusing Axioskop microscope (Carl Zeiss, Thornwood, NY), as shown in Fig. 2. Our Mira 900 Ti:sapphire ultrafast laser (Coherent, Santa Clara, CA) is pumped by a 10 W Verdi doubled solid-state laser (Coherent). Mirrors direct the beam into the Fluoview scan-head, first passing through a Pockels cell (350-160 controlled by Conoptics 25D, Conoptics, Danbury, CT) to modulate the beam intensity and then half- and quarter-waveplates (CVI Laser ACWP-700-1100-10-2 and CVI Laser QWPO-870-10-4) to produce circularly polarized light at the sample. We direct the scanning beam from the Fluoview into the Axioskop from above, passing through a planoconcave, $f = -150$ mm, BK7 lens (KPC031AR.16, Newport, Irvine, CA) to ensure that the bright-field focus and the focus for nonlinear excitation are colocalized for the objective used in our experiments. For nonlinear (simultaneous SHG and 2PF) imaging mode, an infinity-corrected 40×0.8 NA water-immersion objective (Zeiss IR-Achroplan) focuses the ultrafast beam into the sample. The objective has a working distance of 3.6 mm. 2PF is collected by the objective, passed through filters to select emission wavelengths of interest

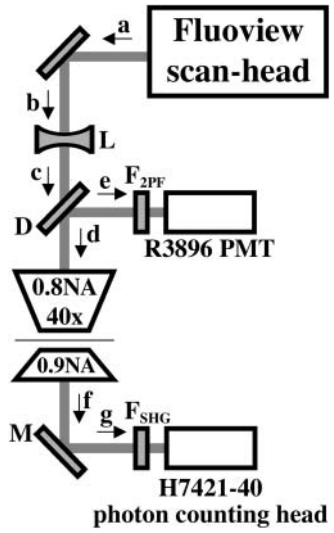

FIGURE 2 Schematic of our nonlinear microscope. Excitation light leaves (*a*) the scan-head and is directed (*b*) through the diverging lens (*L*) into the microscope. The light passes (*c*) through the dichroic (*D*) to enter (*d*) the objective. 2PF is collected back through the objective and the dichroic reflects it (*e*) through filters for 2PF wavelengths (F_{2PF}) into the photomultiplier tube. The condenser collects all transmitted light, directing it (*f*) to the mirror (*M*), selectively reflecting SHG (*g*) through filters for the SHG wavelength (F_{SHG}) into the photon-counting head.

and directly detected by a photomultiplier tube (R3896, Hamamatsu, Bridgewater, NJ) connected to the Fluoview amplifier board (Olympus F5-PSU-B). In these experiments, we used two dichroics (*D* in Fig. 2), one for excitation wavelengths up to 910 nm and another for wavelengths longer than 910 nm. Second harmonic light is produced in the forward direction and is collected using a 0.9 NA condenser (Zeiss), then reflected from a band-reflecting mirror selected for the appropriate second harmonic wavelength (*M* in Fig. 2) to focus through appropriate filters onto a photon-counting head (Hamamatsu H7421-40). See the tables in Supplemental Material for specifications of the detection optics used in this work.

Cells

We grow N1E-115 mouse neuroblastoma cells in Dulbecco's modified Eagle's medium with 10% fetal bovine serum and 1% antibiotic-antimycotic (all from Invitrogen, Carlsbad, CA) and maintained at 37°C with 5% CO_2. During experiments, we used an external buffer consisting of 20 mM HEPES (Calbiochem-Novabiochem AG, now Merck Biosciences AG, Laufelfingen, Switzerland) in Earle's balanced salt solution (EBSS, Sigma, St. Louis, MO) and an internal patch pipette buffer consisting of potassium aspartate (Sigma) at 140 mM, sodium chloride (Sigma) at 5 mM and HEPES at 10 mM, adjusted to pH 7.35 by stock potassium hydroxide and hydrochloric acid solutions.

For patching and imaging, we transferred each 22-mm round cover glass (12-546-1, Fisher Scientific, Pittsburgh, PA) with adherent neuroblastoma cells into a 60 mm plastic dish (353002, Becton Dickinson, Franklin Lakes, NJ) with the sides trimmed down two-thirds of the way around to allow access by patch pipettes and switching between air and water objectives. We held the cover glass in place with small spots of vacuum grease and then added 3 mL external buffer.

Staining

We prepared dyes using procedures adapted from Hassner et al. (1984), as detailed in Supplemental Material, and we characterized their 1PF properties

using a hemispherical lipid bilayer (HLB) apparatus (Loew et al., 1979; Loew and Simpson, 1981). We prepared aqueous solutions of dye in complex with cyclodextrin to facilitate and accelerate staining (Bullen and Loew, 2001). We first dissolved the dye in 100% ethanol at 4 mM, then diluted it by a factor of 20 with 20 mM carboxyethyl-γ-cyclodextrin (CE-γ-CD) (TCEG, Cyclodextrin Technologies Development, High Springs, FL) in distilled water. We dehydrated 0.5-mL aliquots of this mixture in a rotary vacuum evaporator (SS31, Savant Instruments, Holbrook, NY), stored the portions dry and then reconstituted the solution for use in experiments, using 1 mL external buffer to provide an aqueous dye solution at 100 μM. Once a good whole cell patch was obtained, we added 0.1 mL dye/CE-γ-CD to the dish for a final dye concentration of ~3 μM. In the complexed form, the dye dispersed rapidly throughout the buffer, quickly staining the cells in the dish, so we started imaging immediately.

Electrophysiology

For voltage clamping, we controlled a patch-clamp amplifier (BC-525C, Warner Instruments, Hamden, CT) with a computer running our own software in LabVIEW (National Instruments, Austin, TX). The software provided diagnostics such as seal resistance during patching and synchronization of voltage switching with nonlinear imaging, using pin 5 (vertical sync) of the trigger (EXT-TRG) output of the Fluoview. We pulled patch pipettes on a Brown-Flaming micropipette puller (P-80, Sutter Instrument, Novato, CA) from 1.5 mm outer diameter, 0.86 mm inner diameter borosilicate glass (BF150-86-10, Sutter Instrument) and had a resistance of ~6 MΩ when filled with internal buffer. Using the air objective and bright-field imaging, we selected single cells having no physical contact with other cells for patching to a gigaohm seal (Penner, 1995). The intact patches were more stable than the whole cell patches used for voltage clamping, and so we switched the configuration of the microscope from bright-field imaging to nonlinear imaging before forming the whole-cell patch, after which the cells were stained. We set up each experiment to take a series of 27 images with the clamp voltage switched back and forth between 0 mV and a test voltage after every three image frames.

We obtained numerical data from each series of 27 images by selecting the pixels associated with the cell membrane and summing the intensity values of those pixels for each frame in the image sequence, $I.(t_i)$ for i from 1 to 27. For each channel, 15 total intensity values, $I_0(t_i)$, correspond to the 0-mV reference voltage and 12 values, $I_V(t_i)$, correspond to the test voltage, V. Since the $I_0(t_i)$ and $I_V(t_i)$ drift somewhat over time, we normalized all of the $I.(t_i)$ by a second-order polynomial, $A_0(t_i)$, that was fit to the 15 $I_0(t_i)$. The normalized total intensity values $N.(t_i)$ are then just $I.(t_i)/A_0(t_i)$ for each i and the average relative signal change for the test voltage is $\langle N_V(t_i)\rangle - \langle N_0(t_i)\rangle$. This average relative signal change is considered a single experimental measurement, though it should be noted that each measurement obtained in this way actually represents data collected over an entire cell membrane and averaged over 15 0-mV images and 12 test-voltage images.

RESULTS

SHG and 2PF images of a typical neuroblastoma cell stained with di-4-ANEPPS and excited at 910 nm are shown in Fig. 3. We patched and stained this cell as described in Materials and Methods. Though we did not generally use on-the-fly averaging while obtaining image series, each image in Fig. 3 is a Kalman average of three acquisitions in order to yield a cleaner visual presentation. Histograms of membrane pixel intensities (not shown) indicate that, even with averaging, the SHG channel shows more noise with a wider range of intensities than the 2PF channel. On the basis of previous

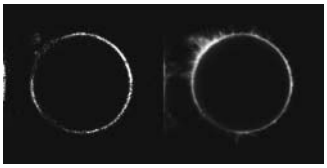

FIGURE 3 Simultaneously acquired SHG (*left*) and 2PF (*right*) images of an N1E-115 mouse neuroblastoma cell stained with ~3 μM di-4-ANEPPS and excited at 910 nm; 2PF was collected between 430 nm and 615 nm. Each image is a Kalman average of three acquisitions. This cell is patched, with the pipette entering the field of view from the lower left corner and resulting in a reduction in membrane SHG and 2PF in the lower left quadrant.

experiments and calculations (Campagnola et al., 1999; Millard et al., 2003a) we may estimate that a typical pixel intensity under second-harmonic imaging microscopy of a cell stained with di-4-ANEPPS corresponds to ~5 photons, whereas we estimate that the photon rate for 2PF is ~400× greater, reducing photon noise correspondingly; see Supplemental Material for the details of this estimation. Also note that the filopodia appearing in the 2PF image are sufficiently small that the opposing membranes are within the optical coherence length of ~λ/10 (Campagnola et al., 2002); thus, the noncentrosymmetric constraint is violated and the filopodia do not appear in the SHG image. The reduction in membrane SHG in the upper left quadrant of the cell may be related to the density of filopodia there.

As described in Materials and Methods, our protocol for determining the voltage sensitivity of 2PF and SHG involved recording a series of 27 images, the clamp voltage being switched between 0 mV and the test voltage V after every three images in each series. The total intensity values, $I.(t_i)$, are shown for a sample image series taken at 910 nm and with $V = -100$ mV in Fig. 4. It can be seen that, in addition to scatter, the $I_0(t_i)$ and $I_V(t_i)$ drift over time, due to a small continued incorporation of dye into the membrane during the course of the experiment. We have found that it is easier to work with cells that are stained after patching, rather than with prestained cells, and the dye/carboxyethyl-γ-cyclodextrin complex is a more efficient method of staining than methods that employ surfactants (Lojewska and Loew, 1987) such as Pluronic F-127 (Molecular Probes, Eugene, OR, P-6867). Although methyl-β-cyclodextrin extracts cholesterol from cell membranes (Simons and Toomre, 2000) we have seen no evidence that carboxyethyl-γ-cyclodextrin affects cells. The normalized total intensity values, $N.(t_i)$, are shown in Fig. 5, demonstrating that our normalization process successfully corrects for the drift. The average relative signal change for this sample image series is (32.0 ± 1.4)%, representing data collected over an entire cell membrane and averaged over 15 images recorded at 0 mV and 12 images recorded at −100 mV.

To illustrate SHG signal changes visually, we processed an SHG image series (of which Fig. 3 shows a single frame), as described in Materials and Methods, to produce the

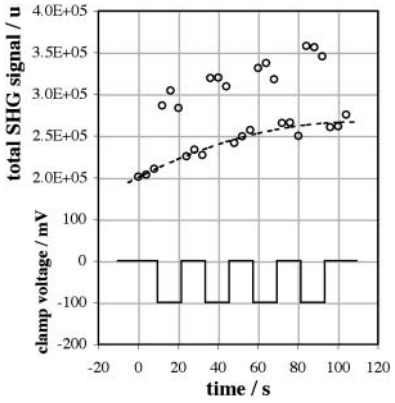

FIGURE 4 Raw data (*circles*, *upper left axis*) obtained from totaling SHG intensity values of pixels associated with the membrane of a voltage-clamped N1E-115 mouse neuroblastoma cell, stained with ~3 μM di-4-ANEPPS and excited at 910 nm. Each point is the total membrane signal for SHG from one frame of the image series. The dashed line shows the interpolated moving average, $A_0(t_i)$, as described in the text. The voltage clamp (*solid line*, *lower left axis*) is cycled between 0 mV and −100 mV with three frames acquired at each voltage.

montage shown in Fig. 6. Modulation of SHG intensity by TMP is clear. Note that these images are the first 15 of the 27 images in the series. In this case, each recorded image is a Kalman average of three acquisitions, so as to improve signal-to-noise for display purposes. These 81 acquisitions, each corresponding to an ~2.5-s acquisition time, took place without any major degradation in SHG intensity and with a stable response to the step changes in TMP. Such stability appears to be dependent on excitation wavelength, with greater degradation of both SHG and 2PF intensity at wavelengths <830 nm—attempts to image at 780 nm, for instance, typically result in rapid, readily visible damage (Campagnola et al., 1999)—along with gradual loss of cell viability with increased light exposure.

Fig. 7 shows relative signal changes in SHG and 2PF versus clamp voltage for di-4-ANEPPS at 850 nm. Both curves have been fit with a straight line going through the origin. Fig. 8 shows relative signal changes versus clamp voltage for the same dye at 910 nm.

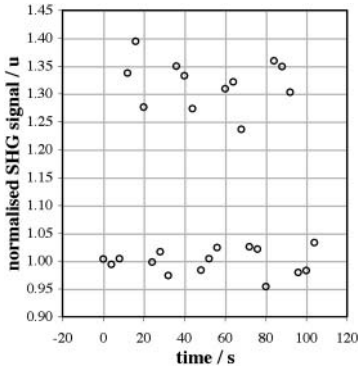

FIGURE 5 Data points from Fig. 4 normalized by the interpolated moving average $A_0(t_i)$ calculated from the 0 mV values. The SHG signal change calculated from this series is (32.0 ± 1.4)%.

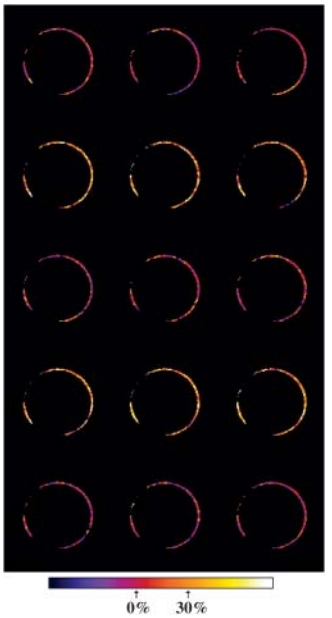

FIGURE 6 SHG images (processed as described in Supplemental Material) of the same cell shown in Fig. 3 at 0 mV (first, third, and fifth rows) and at −100 mV (second and fourth rows). The color bar shows levels corresponding to the normalized reference intensity (marked 0%) and to a normalized intensity 30% above the reference. The average relative signal change for this image series is (27.0 ± 2.6)%.

We define the voltage sensitivity, either for SHG or 2PF (or 1PF), as the slope of the linear fit for signal change relative to the 0 mV intensity. We shall express a voltage sensitivity calculated in this way as a percentage change per 100 mV. From the linear fit shown in Fig. 7, the voltage sensitivity at 850 nm is (−18.5 ± 0.5)%/100 mV for SHG (on the basis of a total of 38 image sequences using ~30 cells) and ~6.6%/100 mV for 2PF. From the fit shown in

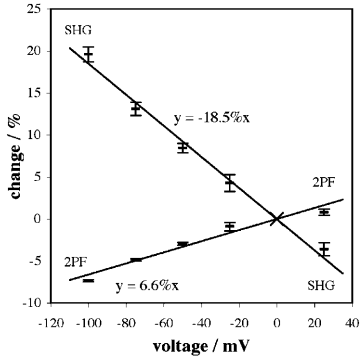

FIGURE 7 Signal changes versus voltage for 850 nm excitation of SHG and 2PF from di-4-ANEPPS. Each data point indicates the mean change for a number of measurements; each error bar in this and subsequent plots shows the standard error of the mean. 2PF was collected for wavelengths between 490 nm and 560 nm.

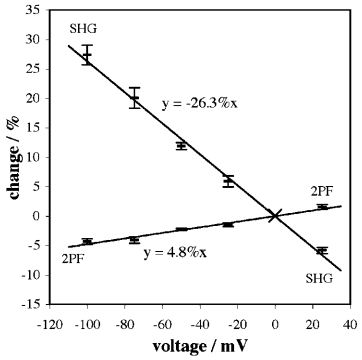

FIGURE 8 Signal changes versus voltage for 910 nm excitation of SHG and 2PF from di-4-ANEPPS. 2PF was collected for wavelengths between 490 nm and 560 nm.

Fig. 8, the voltage sensitivity at 910 nm is (−26.3 ± 0.8)%/100 mV for SHG (on the basis of 52 image sequences using ~40 cells) and ~4.8%/100 mV for 2PF. We therefore find that the voltage sensitivity of SHG from di-4-ANEPPS is increased by ~42% between 850 nm and 910 nm, whereas the voltage sensitivity of 2PF is reduced by ~27%.

Fig. 9 shows the actual changes for −50 mV relative to 0 mV for excitation wavelengths between 830 nm and 970 nm. (Shorter wavelengths damage the cells too quickly while our present laser system will not mode-lock beyond 985 nm.) The ''fits'' are meant only as a visual aid, but there is clearly an increase of the voltage sensitivity of SHG above 890 nm. This is good evidence for a two-photon resonance (Williams, 1984) corresponding to the 465 nm one-photon absorption maximum of di-4-ANEPPS in lipid—the quantum mechanical selection rules are different for two-photon processes compared with one-photon processes such that two-photon spectra rarely map exactly to one-photon spectra through a simple halving of excitation wavelength. Although it would be desirable to collect data at even longer excitation wavelengths, the data shown in Fig. 9 suggests that the peak of the SHG voltage sensitivity lies in the range 960–980 nm, with the maximum value being ~38%/100 mV. On two occasions, one at 950 nm and the other at 970 nm, we measured signal changes of greater than 20% for a voltage change of −50 mV, and then applying a voltage change of −100 mV to the same cells, we measured signal changes of (43.4 ± 2.6)% and (41.6 ± 1.3)%, respectively. For comparison, the voltage sensitivity at optimal excitation and emission wavelengths for 1PF from di-4-ANEPPS, as determined by the HLB apparatus, is ~10%/100 mV.

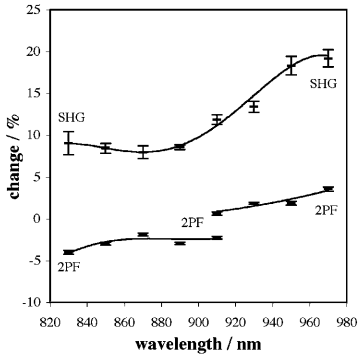

FIGURE 9 Signal changes for 0 mV → −50 mV versus wavelength for SHG and 2PF from di-4-ANEPPS. The arbitrary fits are intended for trend visualization only. The 2PF data for excitation wavelengths of 830–910 nm was obtained from 2PF detection for wavelengths between 490 nm and 560 nm, whereas the 2PF data for 910–970 nm was obtained from 2PF detection between 430 nm and 615 nm. (Though this wavelength range includes the SHG wavelength, there is essentially no back-scattered SHG on the 2PF channel.) The difference in sign for 2PF changes from the two wavelength ranges indicates that the 2PF emission exhibits a biphasic response similar to that of 1PF emission (Fluhler et al., 1985), a characteristic consistent with an electrochromic mechanism for voltage sensitivity.

Fig. 10 shows the SHG and 2PF changes for −50 mV relative to 0 mV at 850 nm for di-4-ANEPPS, di-4-ANEPMRF and di-4-ANEPMPOH. For comparison, 1PF changes measured on the HLB apparatus for −50 mV relative to 0 mV were ~5%, ~2%, and ~0.8%, respectively, at their optimal excitation and emission wavelengths. These molecules differ only in the moiety attached to the pyridinium nitrogen, yet such structural changes clearly affect their voltage sensitivities, though not in the same way for SHG versus 2PF versus 1PF. Fig. 11 shows the equivalent SHG and 2PF changes for 910 nm. In all three cases, the SHG change is increased by going to the longer excitation wavelength (by ~41%, ~143%, and ~17%, respectively) whereas the 2PF change is reduced (by ~23%, ~15%, and ~40%, respectively). Note that not only is the voltage sensitivity different for the different dyes, but the exact dependence on excitation wavelength is also different. The SHG and 2PF sensitivities of di-4-ANEPMRF are increased for the longer wavelength relative to the sensitivities of di-4-ANEPPS, whereas for di-4-ANEPMPOH both sensitivities are decreased.

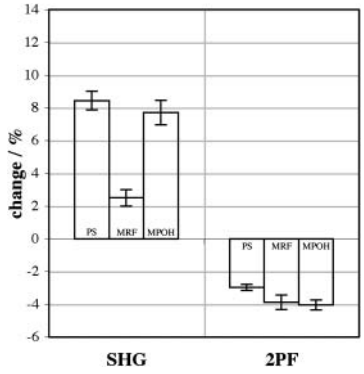

FIGURE 10 Signal changes for 0 mV → −50 mV for 850 nm excitation of SHG and 2PF from di-4-ANEPPS, di-4-ANEPMRF, and di-4-ANEPMPOH. 2PF was collected for wavelengths between 490 nm and 560 nm.

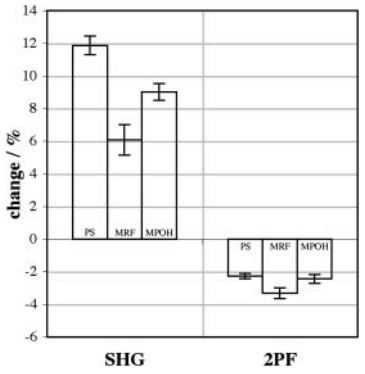

FIGURE 11 Signal changes for 0 mV → −50 mV for 910 nm excitation of SHG and 2PF from di-4-ANEPPS, di-4-ANEPMRF, and di-4-ANEPMPOH. 2PF was collected for wavelengths between 490 nm and 560 nm.

DISCUSSION

In our investigation of the voltage sensitivity of SHG from styryl dyes, we use voltage clamping of live cells to control TMP in a well-defined manner. For di-4-ANEPPS and di-4-ANEPMPOH we have measured voltage sensitivities of ~20%/100 mV at 850–910 nm. For di-4-ANEPPS we have identified significant resonance enhancement at 950–970 nm, producing voltage sensitivities up to ~40%/100 mV, four times better than the nominal voltage sensitivity under 1PF. SHIM clearly has great promise for allowing considerable improvements over existing fluorescence-based techniques to monitor TMP.

It is helpful to put our results in the context of earlier measurements of SHG as a function of TMP for ANEP-based dyes. The first such measurements (Bouevitch et al., 1993) used HLBs of oxidized cholesterol stained with dye. A nonimaging, phase-locked integrator scheme was used to measure signal changes when switching between ±20 mV, and the excitation wavelength from a Q-switched Nd:YAG laser was 1064 nm. Using our definition of voltage sensitivity as the signal change relative to the 0 mV intensity, Bouevitch et al. found sensitivities of (22 ± 8)%/100 mV for di-4-ANEPMPOH, (28 ± 9)%/100 mV for di-4-ANEPMRF and (22 ± 9)%/100 mV for di-2-ANEPMPOH. The same HLB system was later used (Ben-Oren et al., 1996) for a more thorough characterization of SHG from di-2-ANEPMPOH at a number of voltages up to 250 mV, refining the measurement of voltage sensitivity to ~19%/100 mV. These sensitivities compare well with those we have measured away from the peak of resonance enhancement.

Two later sets of measurements (Campagnola et al., 1999; Peleg et al., 1999) used the indirect method of cell depolarization by increasing extracellular potassium and apparently found voltage sensitivities an order of magnitude larger than either the HLB measurements or our voltage-clamping measurements. Though redistributing dyes such as TMRE (Ehrenberg et al., 1988; Loew, 1999) reliably measure membrane depolarization resulting from an increase in extracellular potassium, we believe that other parameters of the dye-membrane system are affected by the potassium, in turn affecting SHG. Thus potassium-induced depolarization is not as well controlled as voltage clamping, allowing for nonvoltage-dependent sources of signal change; see Supplemental Material for further discussion.

Finally, there are a number of possible avenues for future work in this area, which we list here for consideration. 1), As a useful experimental technique, we are seeing excellent sensitivities—from twice to four times those of conventional fluorescence techniques—but signal-to-noise stands to be improved. We typically use the minimum possible excitation intensity that still allows us to obtain reasonable images, since the combination of ultrashort-pulse illumination, staining, and voltage clamping at hyperpolarizing TMPs appears to induce cell damage. However, there are ways in which the technique could be improved, perhaps with the use of ATP and/or antioxidant solutions, to mitigate photodamage. 2), In addition to the electric field arising from the TMP, there is a contribution to the electric field by the dipole potential close to the surface of the membrane. The electric field just inside the membrane may be as intense as 1 GV m^{-1} (Gross et al., 1994), significantly greater than the ~20 MV m^{-1} contribution of the TMP alone. It is known, for instance, that modification of the dipole potential through such compounds as 6-ketocholestanol and phloretin (Gross et al., 1994), variations in the dipole potential due to differences in lipid composition (Bedlack et al., 1994), and changes in the dipole potential following activation of phospholipase C (Xu and Loew, 2003) can be detected by 1PF imaging and spectroscopy and should affect SHG. 3), SHG depends quadratically on staining concentration and it is possible that SHG voltage sensitivity may be affected by concentration. It is known that dye molecules affect one another, as shown by self-quenching and the shifting of absorption and emission spectra. Consistent with their electrochromism, the dyes are also solvatochromic (Pevzner et al., 1993), with behavior of bulk dye different from that of dye-in-lipid. Since the dipole potential in the vicinity of the dye molecule depends on local membrane constituents, including lipids, proteins, and other dye molecules, it seems reasonable to assume that voltage sensitivity may depend on staining. The dependence of voltage sensitivity on staining concentration has not yet been investigated, though it is not likely to be a very strong effect. 4), It is clear that voltage sensitivity depends on the structure of the whole dye, not just on the chromophore, and greater voltage sensitivities may be obtained through rational dye design and modification. We have found that voltage sensitivity can be strongly affected by the structure of the moiety attached to the pyridinium nitrogen of the chromophore. Raman spectroscopy confirms

that this moiety protrudes from the lipid environment of the membrane, demonstrating spectral sensitivity to the extracellular medium (Pevzner et al., 1993). There are also highly conjugated yet nonfluorescent dyes, such as carotenoids and porphyrins, that produce excellent third harmonic generation (Millard et al., 1999) and such dyes that have asymmetric molecular structures may be useful for SHG imaging and SHG voltage sensing.

SUPPLEMENTARY MATERIAL

An online supplement to this article can be found by visiting BJ Online at http://www.biophysj.org.

The authors thank Dr. Heather A. Clark, Dr. David Boudreau, and Prof. Paul L. Campagnola for their help and encouragement concerning all aspects of this work. A.C.M thanks D.B. for the drawings of chemical structures. We would also like to thank James Schaff and Dr. Ion Moraru for discussions concerning visual presentation of cell images.

We gratefully acknowledge financial support under Office of Naval Research grant N0014-98-1-0703, National Institutes of Health, National Institute of Biomedical Imaging and Bioengineering grant R01EB00196.

REFERENCES

Bedlack, R. S., M.-D. Wei, S. H. Fox, E. Gross, and L. M. Loew. 1994. Distinct electric potentials in soma and neurite membranes. *Neuron*. 13:1187–1193.

Ben-Oren, I., G. Peleg, A. Lewis, B. Minke, and L. M. Loew. 1996. Infrared non-linear optical measurements of membrane potential in photoreceptor cells. *Biophys. J*. 71:1616–1620.

Bouevitch, O., A. Lewis, I. Pinevsky, J. P. Wuskell, and L. M. Loew. 1993. Probing membrane potential with nonlinear optics. *Biophys. J*. 65:672–679.

Boyd, R. W. 1992. Nonlinear Optics. Academic Press, San Diego.

Bullen, A., and L. M. Loew. 2001. Solubility and intracellular delivery of hydrophobic voltage-sensitive dyes with chemically-modified cyclodextrins. *Biophys. J*. 80:168a (Abstr.).

Campagnola, P. J., A. C. Millard, M. Terasaki, P. E. Hoppe, C. J. Malone, and W. Mohler. 2002. Three-dimensional high-resolution second-harmonic generation imaging of endogenous structural proteins in biological tissues. *Biophys. J*. 82:493–508.

Campagnola, P. J., M.-D. Wei, A. Lewis, and L. M. Loew. 1999. High-resolution nonlinear optical microscopy of living cells by second harmonic generation. *Biophys. J*. 77:3341–3349.

Cohen, L. B., B. M. Salzberg, H. V. Davila, W. N. Ross, D. Landowne, A. S. Waggoner, and C. H. Wang. 1974. Changes in axon fluorescence during activity: molecular probes of membrane potential. *J. Membr. Biol*. 19:1–36.

Ehrenberg, B., V. Montana, M.-D. Wei, J. P. Wuskell, and L. M. Loew. 1988. Membrane potential can be determined in individual cells from the nernstian distribution of cationic dyes. *Biophys. J*. 53:785–794.

Eisenthal, K. B. 1996. Liquid interfaces probed by second harmonic and sum frequency spectroscopy. *Chem. Rev*. 96:1343–1360.

Fluhler, E., V. G. Burnham, and L. M. Loew. 1985. Spectra, membrane binding and potentiometric responses of new charge-shift probes. *Biochemistry*. 24:5749–5755.

Freedman, J. C., and P. C. Laris. 1981. Electrophysiology of cells and organelles: studies with optical potentiometric indicators. *Int. Rev. Cytol. Suppl*. 12:177–246.

Gross, E., R. S. Bedlack, and L. M. Loew. 1994. Dual-wavelength ratiometric fluorescence measurement of the membrane dipole potential. *Biophys. J*. 67:208–216.

Hassner, A., D. Birnbaum, and L. M. Loew. 1984. Charge-shift probes of membrane potential: synthesis. *J. Org. Chem*. 49:2546–2551.

Huang, J., Z. Chen, and A. Lewis. 1989. Second harmonic generation in purple membrane poly(vinyl alcohol) films: probing the dipolar characteristics of the bacteriorhodopsin chromophore in bR_{570} and M_{412}. *J. Phys. Chem*. 93:3314–3320.

Loew, L. M. 1982. Design and characterization of electrochromic membrane probes. *J. Biochem. Biophys. Methods*. 6:243–260.

Loew, L. M. 1999. Potentiometric membrane dyes and imaging membrane potential in single cells. *In* Fluorescent and Luminescent Probes for Biological Activity. W.T. Manson, editor. Academic Press, New York. 210–221.

Loew, L. M., G. W. Bonneville, and J. Surow. 1978. Charge-shift optical probes of membrane potential: theory. *Biochemistry*. 17:4065–4071.

Loew, L. M., L. B. Cohen, J. Dix, E. N. Fluhler, V. Montana, G. Salama, and J. Y. Wu. 1992. A naphthyl analog of the aminostyryl pyridinium class of potentiometric membrane dyes shows consistent sensitivity in a variety of tissue, cell and model membrane preparations. *J. Membr. Biol*. 130:1–10.

Loew, L. M., S. Scully, L. Simpson, and A. S. Waggoner. 1979. Evidence for a charge-shift electrochromic mechanism in a probe of membrane potential. *Nature*. 281:497–499.

Loew, L. M., and L. Simpson. 1981. Charge shift probes of membrane potential: a probable electrochromic mechanism for p-aminostyrylpyridinium probes on a hemispherical lipid bilayer. *Biophys. J*. 34:353–365.

Lojewska, Z., and L. M. Loew. 1987. Insertion of amphiphilic molecules into membranes is catalyzed by a high molecular weight non-ionic surfactant. *Biochim. Biophys. Acta*. 899:104–112.

Millard, A. C., P. J. Campagnola, W. Mohler, A. Lewis, and L. M. Loew. 2003a. Second harmonic imaging microscopy. *Methods Enzymol*. 361: 47–69.

Millard, A. C., L. Jin, A. Lewis, and L. M. Loew. 2003b. Direct measurement of the voltage sensitivity of second harmonic generation from a membrane dye in patch-clamped cells. *Opt. Lett*. 28:1221–1223.

Millard, A. C., P. W. Wiseman, D. N. Fittinghoff, K. R. Wilson, J. A. Squier, and M. Müller. 1999. Third harmonic generation microscopy by use of a compact, femtosecond fiber laser source. *Appl. Opt*. 38:7393–7397.

Moreaux, L., T. Pons, V. Dambrin, M. Blanchard-Desce, and J. Mertz. 2003. Electro-optic response of second harmonic generation membrane potential sensors. *Opt. Lett*. 28:625–627.

Moreaux, L., O. Sandre, M. Blanchard-Desce, and J. Mertz. 2000a. Membrane imaging by simultaneous second harmonic generation and two-photon microscopy. *Opt. Lett*. 25:320–323.

Moreaux, L., O. Sandre, and J. Mertz. 2000b. Membrane imaging by second harmonic generation microscopy. *J. Opt. Soc. Am. B*. 17:1685–1694.

Peleg, G., A. Lewis, M. Linial, and L. M. Loew. 1999. Nonlinear optical measurement of membrane potential around single molecules at selected cellular sites. *Proc. Natl. Acad. Sci. USA*. 96:6700–6704.

Penner, R. 1995. A practical guide to patch clamping. *In* Single-Channel Recording. B. Sakmann and E. Neher, editors. Plenum Press, New York. 3–30.

Pevzner, E., B. Ehrenberg, and L. M. Loew. 1993. On the membrane binding of the potentiometric probe di-4-ANEPPS: a fluorescence and resonance Raman study. *Spectrosc. Lett*. 26:1181–1193.

Shen, Y. R. 1984. The Principles of Non-Linear Optics. John Wiley & Sons, New York.

Shen, Y. R. 1989. Surface properties probed by second harmonic and sum frequency generation. *Nature*. 337:519–525.

Sheppard, C. J. R., R. Kompfner, J. Gannaway, and D. Walsh. 1977. Scanning harmonic optical microscope. *IEEE J. Quantum Elect.* 13E:100D.

Simons, K., and D. Toomre. 2000. Lipid rafts and signal transduction. *Nat. Rev. Mol. Cell Biol.* 1:31–41.

Tasaki, I. 1974. Energy transduction in the nerve membrane and studies of excitation processes with extrinsic fluorescence probes. *Ann. N. Y. Acad. Sci.* 227:247–267.

Williams, D. J. 1984. Organic polymeric and non-polymeric materials with large optical non-linearities. *Angew. Chem. Int. Ed. Engl.* 23:690–703.

Xu, C., and L. M. Loew. 2003. Activation of phospholipase C increases intramembrane electric fields in N1E–115 neuroblastoma cells. *Biophys. J.* 84:4144–4156.

Zhang, J., R. M. Davidson, M. D. Wei, and L. M. Loew. 1998. Membrane electrical properties by combined patch clamp and fluorescence ratio imaging in single neurons. *Biophys. J.* 74:48–53.